

# Ring patterns and their stability in 2D kinematic particle aggregation models

Theodore Kolokolnikov<sup>\*</sup>, Hui Sun<sup>†</sup>, David Uminsky<sup>†</sup>, Andrea L. Bertozzi<sup>†</sup>

<sup>\*</sup>*Department of Mathematics and Statistics, Dalhousie University, Halifax, Canada and*

<sup>†</sup>*Department of Mathematics, UCLA, Los Angeles, CA 90095, USA*

(Dated: August 22, 2010)

We consider a kinematic particle interaction model with broad applications ranging from insect swarms to self-assembly of nanoparticles. With very simple pairwise interaction models possessing both attraction and repulsion, we show a suite of complex 2D ring-like patterns, many of which have not been documented in the literature. Emergence of these patterns is explained by a stability analysis of the ring, involving a reformulation of the problem through a continuum limit in which the particles are concentrated along a curve. Stability of ring states is understood by a linear well-posedness theory for the continuum ring solutions.

PACS numbers: 87.18.Ed, 87.10.Ed, 05.45.-a

In this letter we consider a two-dimensional kinematic model of pairwise particle interaction of the form

$$\frac{dx_j}{dt} = \frac{1}{N} \sum_{\substack{k=1, \dots, N \\ k \neq j}} F(|x_k - x_j|) \frac{x_k - x_j}{|x_k - x_j|}, \quad j = 1 \dots N. \quad (1)$$

This basic model appears in many contexts such as insect aggregation [3], locust swarms [4], and self-assembly of nanoparticles [5]. In one dimension, it includes the Kuramoto model with zero natural frequency [7], as a special case. In the context of locust swarms, the basic principle that keeps the swarm shape is the attractive-repulsive nature of the interaction force  $F(r)$ : the insects repel each other if they are too close, but attract each other at a distance. Mathematically, this corresponds to  $F(r)$  being positive for small  $r$ , but negative for large  $r$ . Commonly, a Morse interaction force of the form

$$F(r) = \exp(-r) - G \exp(-r/L); \quad G < 1, L > 1 \quad (2)$$

has been used [4]; the conditions  $G < 1$  and  $L > 1$  guarantee the attractive-repulsive nature of  $F(r)$ . In the limit  $N \rightarrow \infty$ , two types of behaviour are possible: either a swarm cloud spreads until its area is proportional to  $N$ , or else the swarm radius is bounded independent of  $N$  and forms a well-defined bounded steady state in the continuous limit  $N \rightarrow \infty$  [4]. The latter corresponds to the catastrophic regime of the H-stability diagram [4], [8], [6]. In one dimension, the catastrophic regime occurs when  $GL^2 > 1$  [4], while in two dimensions, the critical threshold is  $GL^3 > 1$  [8].

In this letter we consider what happens for interaction forces where the attraction is much stronger than that of the Morse force. For concreteness, we consider two different families of interaction forces: the simple power force

$$F(r) = r^p - r^q; \quad 0 \leq p < q \quad (3)$$

and an interaction force which consists of a tanh connection of the states  $b \pm 1$ :

$$F(r) = \tanh((1-r)a) + b; \quad 0 < a; \quad -1 < b < 1. \quad (4)$$

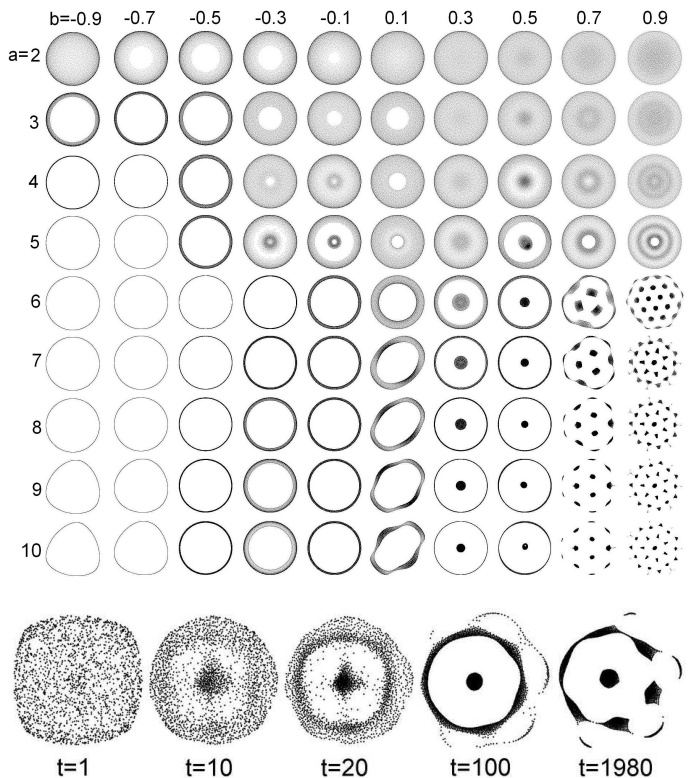


FIG. 1: Top: Long-time behavior of the particle system (1) with  $F(r) = \tanh((1-r)a) + b$  with values of  $a, b$  as indicated. Bottom: time evolution of (1) with  $a = 8, b = 0.67$ .

Unlike the Morse force (2), both (3) and (4) have very strong attraction for large  $r$ ; as a result one can show that the system is in the catastrophic regime and the solution is bounded as  $N \rightarrow \infty$ . On the other hand, steady states can exhibit a very intricate structure as illustrated in Figure 1, for the case  $F(r) = \tanh((1-r)a) + b$ . Starting with random initial conditions, a simple forward Euler time method was used to simulate (1) with  $N = 5000$ . The output is shown at time  $t = 1000$  after 2000 steps.

The long time stable pattern does not appear to be sensitive to initial conditions (up to rotation/translation). Also as expected in the catastrophic regime, doubling the  $N$  does not change the structure or the spatial extend of the steady state. Note the complex patterns ranging from rings and annuli to more complex structures exhibiting period two and three symmetry breaking to very complex ‘soccer ball’ like shapes. We note that related complex patterns (in particular the annuli and spotted patterns) been observed in experiments of stressed bacterial colonies [9] which have associated related nonlocal models [10].

Unlike the Morse interaction force, the force (3) may lead to a steady state which concentrates on a curve. Such a curve often evolves into a circle steady-state, which corresponds to particles aligned uniformly along a ring. Even for more complicated steady states, a ring structure is often seen in the intermediate dynamics, as shown in Figure 2. The existence as well as stability of such a ring solution is therefore important in understanding swarm formation for general interaction forces.

For solutions concentrating on curves and in the limit  $N \rightarrow \infty$ , it is shown in [1] that such curve obeys an evolution law

$$\rho_t = -\rho \frac{\langle z_\alpha, z_{\alpha t} \rangle}{|z_\alpha|^2}; \quad z_t = K * \rho \quad (5)$$

where  $z(\alpha; t)$  is a parametrization of the solution curve;  $\rho(\alpha; t)$  is its density and

$$K * \rho = \int F(|z(\alpha') - z(\alpha)|) \frac{z(\alpha') - z(\alpha)}{|z(\alpha') - z(\alpha)|} \rho(\alpha', t) dS(\alpha'). \quad (6)$$

Note that (5) is a generalization of the classical Birkhoff-Rott equation for gradient vector fields rather than incompressible flow [1, 11].

The ring steady state has the form  $z(\alpha; t) = z(\alpha) = r_0 \exp(i\alpha)$ ,  $\alpha \in [0, 2\pi]$ ; where  $r_0$  is the radius of the ring and must be the root of

$$I(r_0) := \int_0^{2\pi} F(2r_0 \sin \theta) \sin \theta d\theta = 0. \quad (7)$$

For the Morse force (2), note that  $I(0) > 0$  and  $I(r) \sim \frac{1}{4r} (1 - GL^2)$  as  $r \rightarrow \infty$ . It follows that a ring steady state exists provided  $GL^2 > 1$ , which corresponds to the catastrophic regime of the one-dimensional model. For forces (3) and (4), the ring solution exists for all parameter values within the indicated range.

To study the local stability of a ring solution, we consider the perturbations of the ring of  $N$  particles of the form  $x_k = r_0 \exp(2\pi i k/N) (1 + \exp(t\lambda)\phi_k)$  where  $\phi_k \ll 1$ . After some algebra we obtain

$$\lambda \phi_j = \frac{1}{N} \sum_{\substack{k=1, \dots, N \\ k \neq j}} G_1 \left( \frac{\pi(k-j)}{N} \right) \left( \phi_j - \phi_k \exp \left( \frac{2\pi i(k-j)}{N} \right) \right) \\ + G_2 \left( \frac{\pi(k-j)}{N} \right) \left( \bar{\phi}_k - \bar{\phi}_j \exp \left( \frac{2\pi i(k-j)}{N} \right) \right),$$

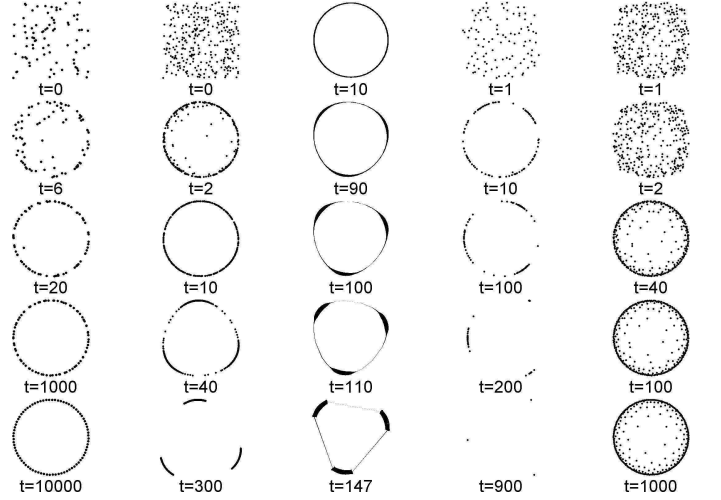


FIG. 2: Dynamics of (1). First column:  $F(r) = r - r^2$ ,  $N = 80$ . The equilibrium solution is a stable ring. Second column:  $F(r) = r^{0.5} - r^6$ ,  $N = 300$ . Third column: Simulation of the continuum limit (5) with  $F$  as in the second column. Fourth column:  $F(r) = r - r^{3.2}$ ,  $N = 100$ . Fifth column:  $F(r) = r^{0.5} - r^{1.5}$ ,  $N = 300$ .

where  $j = 1 \dots N$  and

$$G_1(\theta) = \frac{1}{2} \left( F'(2r_0 |\sin \theta|) + \frac{F(2r_0 |\sin \theta|)}{2r_0 |\sin \theta|} \right) \\ G_2(\theta) = \frac{1}{2} \left( F'(2r_0 |\sin \theta|) - \frac{F(2r_0 |\sin \theta|)}{2r_0 |\sin \theta|} \right).$$

Next we substitute  $\phi_j = b_+ e^{2m\pi i j/N} + b_- e^{-2m\pi i j/N}$  where we assume that  $b_\pm$  are real, and  $m$  is a strictly positive integer. This leads to a 2x2 eigenvalue problem  $\lambda \begin{pmatrix} b_+ \\ b_- \end{pmatrix} = M(m) \begin{pmatrix} b_+ \\ b_- \end{pmatrix}$  where

$$M(m) := \begin{bmatrix} I_1(m) & I_2(m) \\ I_2(m) & I_1(-m) \end{bmatrix}; \quad m = 1, 2, \dots; \quad (8)$$

$$I_1(m) = \frac{2}{N} \sum_{l=1}^{N/2} \left[ \frac{F(2r_0 \sin \frac{\pi l}{N})}{2r_0 \sin \frac{\pi l}{N}} + F' \left( 2r_0 \sin \frac{\pi l}{N} \right) \right] \times \\ \times \sin^2 \left( \left( m+1 \right) \frac{\pi l}{N} \right); \quad (9a)$$

$$I_2(m) = \frac{2}{N} \sum_{l=1}^{N/2} \left[ \frac{F(2r_0 \sin \frac{\pi l}{N})}{2r_0 \sin \frac{\pi l}{N}} - F' \left( 2r_0 \sin \frac{\pi l}{N} \right) \right] \times \\ \times \left[ \sin^2 \left( m \frac{\pi l}{N} \right) - \sin^2 \left( \frac{\pi l}{N} \right) \right]. \quad (9b)$$

Taking the continuous limit  $N \rightarrow \infty$ , we obtain

$$I_1(m) = \frac{2}{\pi} \int_0^{\frac{\pi}{2}} \left[ \frac{F(2r_0 \sin \theta)}{2r_0 \sin \theta} + F'(2r_0 \sin \theta) \right] \times \sin^2((m+1)\theta) d\theta; \quad (10a)$$

$$I_2(m) = \frac{2}{\pi} \int_0^{\frac{\pi}{2}} \left[ \frac{F(2r_0 \sin \theta)}{2r_0 \sin \theta} - F'(2r_0 \sin \theta) \right] \times [\sin^2(m\theta) - \sin^2(\theta)] d\theta. \quad (10b)$$

The ring is linearly stable if the eigenvalues  $\lambda$  of (8) are non-positive for all integers  $m \geq 1$ ; otherwise it is unstable. There are two possible types of instabilities - ones in which the ring is simply *long-wave unstable*, corresponding to an instability of a low order mode (small  $m$ ) but stability of higher order modes. The second type corresponds to ill-posedness of the ring in which the eigenvalues are positive in the  $m \rightarrow \infty$  limit and grow as  $m$  increases. In the latter case the ring completely breaks up and often forms a fully two-dimensional pattern. Such stability analysis is well-known for other types of curve evolutions involving active scalar problems - most notably the classical Kelvin-Helmholtz instability (ill-posedness) of the vortex sheet for the 2D Euler equations [11].

Figure 2 shows some typical evolutionary behaviour of our model. In the first column, the equilibrium solution is a stable ring. Random initial conditions quickly converge to a ring shape ( $t = 20$ ); this is followed by slow dynamics along the ring until equilibrium is achieved by  $t = 10000$ . In column 2 a mode  $m = 3$  instability is triggered on a slower timescale than the initial collapse to a ring shape. The final steady-state is a triangular shape, which retains some of the features of the initial instability. Column 3 is the direct numerical simulation of the continuum equations (5) using the Lagrangian method [1], and using the same parameter values as Column 2. The thickness represents the variable density  $\rho$ . In the fourth column, the ring appears as a transient state, but final equilibrium consists of just three points. Column 5 shows another type of instability, which corresponds to very high modes  $m$ ; the ring solution is not only linearly unstable but also linearly ill-posed; the resulting swarm has a two-dimensional shape.

For interaction force (3), and with  $p = 1, q = 2$  we have

$$\text{tr } M(m) = -\frac{(4m^4 - m^2 - 9)}{(4m^2 - 1)(4m^2 - 9)} < 0, \quad m = 2, 3, \dots$$

$$\det M(m) = \frac{3m^2(2m^2 + 1)}{(4m^2 - 9)(4m^2 - 1)^2} > 0, \quad m = 2, 3, \dots$$

This proves that the **ring pattern corresponding to  $F(r) = r - r^2$  is locally stable**. Moreover, for large  $m$ , the two eigenvalues are  $\lambda \sim -\frac{1}{4}$  and  $\lambda \sim -\frac{3}{8m^2} \rightarrow 0$  as  $m \rightarrow \infty$ . The presence of small eigenvalues implies the existence of slow dynamics near the ring equilibrium.

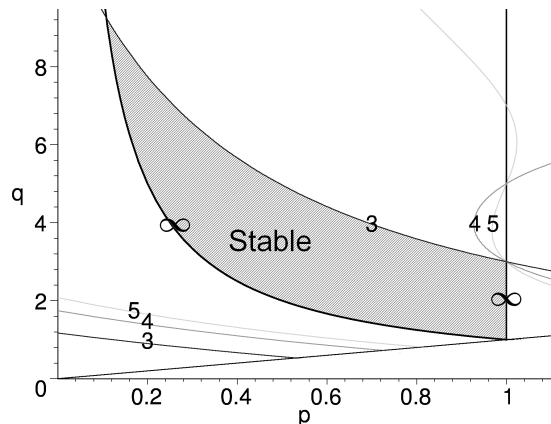


FIG. 3: Stability diagram for (3). The curves shown correspond to the boundaries of the stability  $\det(M(m)) = 0$ , with  $m = 3, 4, 5$  and  $m = \infty$ , as indicated. The line  $p = q$  is also drawn. Crossing any of the curves destabilizes the ring. The intersection of  $m = \infty$  and  $m = 3$  boundaries is at  $p = 0.10779$ ,  $q = 9.277102$ .

Further analysis shows that the eigenvector corresponding to the small eigenvalue and large  $m$  is nearly tangential to the circle; the other eigenvector is nearly perpendicular. The corresponding two-time dynamics are also clearly visible in simulations (Figure 2, column 1).

In general, if  $F(0) > 0$  and  $F$  is  $C^2$ , the asymptotics for large  $m$  yield

$$I_1(m) \sim I_1(-m) \sim \frac{F(0)}{2\pi r_0} \ln m + O(1) \text{ as } m \rightarrow \infty.$$

This shows that  $\text{trace } M(m) > 0$  for sufficiently large  $m$ . It follows that the necessary condition for well-posedness of a ring is that  $F(0) = 0$ . If in addition,  $F$  is  $C^4$ , then using integration by parts we obtain

$$\text{tr } M(m) \sim \frac{2}{\pi} \int_0^{\pi/2} \left( \frac{F(2r_0 \sin \theta)}{2r_0 \sin \theta} - F'(2r_0 \sin \theta) \right) d\theta + O\left(\frac{1}{m^2}\right);$$

$$\det(M(m)) \sim \text{tr } M(m) \frac{F''(0)r_0}{m^2} + O\left(\frac{1}{m^4}\right).$$

In summary, **if  $F(r)$  is  $C^4$  on  $[0, 2r_0]$ , then the necessary and sufficient conditions for well-posedness of a ring are:**

$$F(0) = 0, \quad F''(0) < 0 \quad \text{and} \quad (11)$$

$$\int_0^{\pi/2} \left( \frac{F(2r_0 \sin \theta)}{2r_0 \sin \theta} - F'(2r_0 \sin \theta) \right) d\theta < 0. \quad (12)$$

In particular, **the ring solution for Morse force (2) as well as for forces (4) is always ill-posed**, since  $F(0) > 0$ . Another general result is if  $F$  is odd and  $C^\infty$  on  $[0, 2r_0]$ . In that case, one can show that  $\det(M(m)) = 0$  for all  $m$ ; the ring then has infinitely many zero eigenvalues. This observation may be relevant for the Kuramoto model  $F(r) = \sin(r)$  [7].

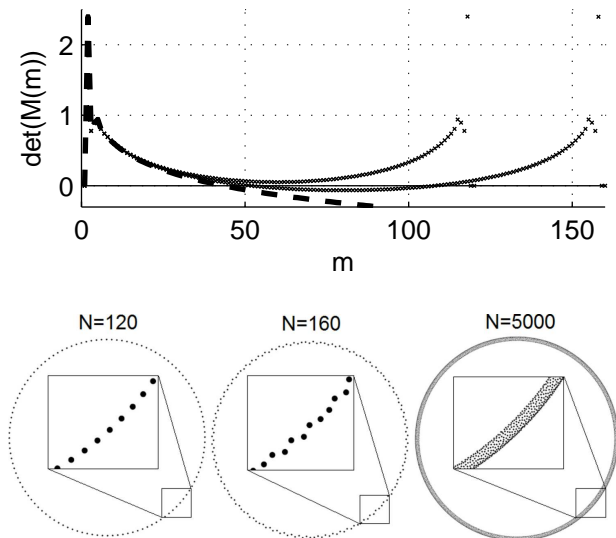


FIG. 4: Stability of discrete vs. continuous system for  $F(r) = \tanh(4(1-r)) - 0.5$ . Top:  $\det(M(m))$ . Dashed line corresponds to continuum eq. (10) and crosses to discrete eq. (9) with  $N = 120, 160$ . Instability occurs iff  $\det(M(m)) < 0$ . Bottom: steady states of discrete dynamics with  $N$  as indicated; inserts show the blowup of the ring structure.

For the force of type (3) with  $0 < p < q$ , the asymptotics of the mode  $m = \infty$  can be computed in terms of Gamma functions. In [2], it is shown that the mode  $m = \infty$  is stable if and only if  $pq > 1$  and  $p < 1$ . In addition, the low modes  $m = 2, 3, 4, \dots$  may also become unstable, see Figure 3. The dominant unstable mode corresponds to  $m = 3$ , which bounds the stability region from above. This boundary is given implicitly by

$$0 = 723 - 594(p + q) - 27(p^2 + q^2) - 431pq \\ + 106(pq^2 + p^2q) + 19(p^3q + pq^3) \\ + 10(p^3q^2 + p^2q^3) + 6(p^3 + q^3) + p^3q^3$$

and is shown in Figure 3. Similarly, the stability boundary for  $m = 2$  mode is given by  $0 = 7 + 38(p + q) + 12pq + 3(p^2 + q^2) + 2(pq^2 + p^2q) - p^2q^2$ ; this boundary happens to lie well outside the area shown in Figure 3. The stability boundaries for modes  $m = 4, 5, \dots$  are also expressed in terms of higher order polynomials in  $p, q$ .

Even if (1) is ill-posed in the *continuous* limit  $N \rightarrow \infty$ , the ring of *discrete* particles (1) may be stable with a relatively large  $N$ . An example of this is shown in Figure 4. Note the slight instability for  $N = 160$  but stability when  $N = 120$ . The continuous limit is well approximated with  $N = 5000$ ; the resulting steady state appears to be a thin annulus, whose inner and outer radius are approximately  $r_0$  given by (7).

Many open questions remain. In a recent work [12], the authors studied the collapse of  $N$  particles into  $K$

points in one dimension, each point having roughly  $N/K$  particles. When  $F(r) = r - r^s$ , they showed that  $N$  particles collapse to two points when  $s \geq 2$ ; no collapse occurs when  $1 < s < 2$ . This is very different than the behaviour in two dimensions: such case corresponds to the edge of the stable region for a ring ( $p = 1$  in Figure 3). A more refined analysis shows that the ring is stable for all  $1 < s < 3$ . Numerics show that the ring collapses into three points when  $s > 3$ .

Another open question is to study the annulus and spot-type solutions, such as shown in Figure 1. These tend to arise in the limit where  $F(r)$  has a sharp transition from repulsive to attractive regime. Unlike the ring solutions discussed above or point solutions of [12], the requirement  $F(0) = 0$  is not necessary.

Numerics suggest that random initial conditions tend to converge to ring solutions, whenever the ring is stable. Global stability of the ring remains an open question.

**Acknowledgements:** T.K. is supported by NSERC grant 47050. D.U. is supported by NSF grant DMS-0902792 and a UC Presidents Fellowship. A.B. and H.S. are supported by NSF grants DMS-0907931 and EFRI-1024765 and ONR grant N000141010641.

- 
- [1] H. Sun, D. Uminsky, A. Bertozzi, in preparation.
  - [2] T. Kolokolnikov, H. Sun, D. Uminsky, A. Bertozzi, in preparation.
  - [3] A. Mogilner, L. Edelstein-Keshet, L. Bent, A. Spiros, J. Math. Biol. 47, 353 (2003); L. Edelstein-Keshet, J. Watmough, D. Grunbaum, J. Math. Biol. 36, 515 (1998).
  - [4] C.M. Topaz, A.J. Bernoff, S. Logan, and W. Toolson, Eur. Phys. J. Special Topics 157, 93–109 (2008); C.M. Topaz, A.L. Bertozzi, and M.A. Lewis, Bull. Math. Biol. 68:1601–1623 (2006); A.J. Leverentz, C.M. Topaz and A.J. Bernoff, SIAM J. Appl. Dyn. Sys. 8(3),880–908 (2009).
  - [5] D. D. Holm and V. Putkaradze, Phys. Rev. Lett. 95, 226106 (2005).
  - [6] D. Ruelle, Statistical Mechanics (Benjamin, New York), 1969.
  - [7] S.H. Strogatz, Physica D 143 (2000) 1–20.
  - [8] M.R. D’Orsogna, Y.L. Chuang, A.L. Bertozzi, and L. Chayes, Phys. Rev. Lett., 96 (2006), paper 104302.
  - [9] L. Tsimring, H. Levine, I. Aranson, E. Ben-Jacob, I. Cohen, O. Shechet, and W. Reynolds, PRL 75(9) 1859 (1995); A. M. Deprato, A. Samadani, A. Kudrolli, and L. S. Tsimring, PRL 87(15) 158102.
  - [10] E. F. Keller and L.A. Segel, J. Theor. Biol., 30:225–234(1971); M.P. Brenner, P. Constantin, L. P. Kadanoff, A. Shenkel and S.C. Venkataramani, Nonlinearity 12:4, 1071–1098(1999); MP Brenner, LS Levitov, EO Budrene, Biophys. J. 74:4, 1677–1693 (1998).
  - [11] R. Krasny, J. Fluid Mech. 167, 65–93 (1986)
  - [12] K. Fellner and G. Raoul, to appear, Math. Models Methods Appl. Sci.